Biochimica et Biophysica Acta 1827 (2013) 248–254

Contents lists available at SciVerse ScienceDirect

Biochimica et Biophysica Acta

journal homepage: www.elsevier.com/locate/bbabio

Carotenoid–protein interaction alters the S_1 energy of hydroxyechinenone in the Orange Carotenoid Protein

Tomáš Polívka [a,b,*], Pavel Chábera [c], Cheryl A. Kerfeld [d,e]

[a] Faculty of Science, University of South Bohemia, Branišovská 31, 370 05 České Budějovice, Czech Republic
[b] Biological Centre, Czech Academy of Sciences, Branišovská 31, 370 05 České Budějovice, Czech Republic
[c] Department of Chemical Physics, Lund University, SE-222 41 Lund, Sweden
[d] Department of Plant and Microbial Biology, University of California, Berkeley, USA
[e] US Department of Energy, Joint Genome Institute, Walnut Creek, CA, USA

ARTICLE INFO

Article history:
Received 10 August 2012
Received in revised form 4 October 2012
Accepted 8 October 2012
Available online 16 October 2012

Keywords:
Photoprotection
Cyanobacteria
Carotenoid
Orange Carotenoid Protein
Femtosecond transient absorption spectroscopy

ABSTRACT

The Orange Carotenoid Protein (OCP) is a photoactive water soluble protein that is crucial for photoprotection in cyanobacteria. When activated by blue-green light, it triggers quenching of phycobilisome fluorescence and regulates energy flow from the phycobilisome to the reaction center. The OCP contains a single pigment, the carotenoid 3′-hydroxyechinenone (hECN). Binding to the OCP causes a conformational change in hECN leading to an extension of its effective conjugation length. We have determined the S_1 energy of hECN in organic solvent and compared it with the S_1 energy of hECN bound to the OCP. In methanol and n-hexane, hECN has an S_1 energy of 14,300 cm^{-1}, slightly higher than carotenoids with shorter conjugation lengths such as zeaxanthin or β-carotene; this is consistent with the proposal that the presence of the conjugated carbonyl group in hECN increases its S_1 energy. The S_1 energy of hECN in organic solvent is independent of solvent polarity. Upon binding to the OCP, the S_1 energy of hECN is further increased to 14,700 cm^{-1}, underscoring the importance of protein binding which twists the conjugated carbonyl group into s-trans conformation and enhances the effect of the carbonyl group. Activated OCP, however, has an S_1 energy of 14,000 cm^{-1}, indicating that significant changes in the vicinity of the conjugated carbonyl group occur upon activation.

1. Introduction

Photoprotection is, along with light-harvesting, the key process taking place in photosynthetic antenna systems [1]. While light-harvesting processes are understood in great detail in many photosynthetic organisms [1–3], the understanding of photoprotective mechanisms remains limited. It is now an established fact that carotenoids are the crucial players in photoprotection. Their ability to quench triplet states of chlorophylls and bacteriochlorophylls and to scavenge deleterious singlet oxygen via triplet–triplet energy transfer is well known [4–6]. However, carotenoids in the photosynthetic systems of plants and algae can also act as 'fast' quenchers; they are able to quench singlet states of Chl-*a* directly in a process known as non-photochemical quenching (NPQ) [7,8].

NPQ is manifested as a decrease of Chl-*a* fluorescence under high-light conditions but the precise molecular mechanism leading to removal of the population of fluorescing Chl-*a* Q_y state is still a subject of debate. There are currently four models suggesting how the excess excited state energy of Chl-*a* is quenched: 1) via energy transfer to the carotenoid S_1 state [9], 2) via electron transfer, resulting in a Chl-*a* anion and a carotenoid cation that recombine on a picosecond time scale [10], 3) it is achieved via carotenoid-Chl exciton coupling that provides a pathway for deactivation of excess excited Chl via the rapidly-decaying S_1 state of the carotenoid [11], and 4) it results from formation of Chl/Chl exciton pairs which undergo charge transfer as the pathway for Chl excited state deactivation. This fourth model does not involve carotenoids directly; they are assumed to trigger formation of the Chl/Chl exciton pairs [12].

Until recently, NPQ has been associated only with plants but a number of studies in the past few years have shown that NPQ also exists in cyanobacteria via two types of energy dissipation. The first takes place through the stress-induced protein IsiA [13]; the other utilizes a 35 kDa water-soluble carotenoid-binding protein known as the Orange Carotenoid Protein (OCP) that is responsible for quenching of phycobilisome fluorescence, thereby regulating energy flow between phycobilisomes, (the main antenna system of cyanobacteria), and PSII [14–19]. The OCP, whose high-resolution (1.65 Å) crystal structure is known [20,21], binds a single pigment, the

* Corresponding author at: Faculty of Science, University of South Bohemia, Branišovská 31, 370 05 České Budějovice, Czech Republic. Tel.: +420 389 032 006; fax: +420 385 310 366.
E-mail address: tpolivka@jcu.cz (T. Polívka).

0005-2728/$ – see front matter © 2012 Elsevier B.V. All rights reserved.
http://dx.doi.org/10.1016/j.bbabio.2012.10.005

carotenoid 3′-hydroxyechinenone (hECN). hECN contains 11 conjugated C=C bonds and is terminated by a carbonyl group that is nestled in a binding pocket in the C-terminal domain of the OCP. The keto oxygen of hECN forms hydrogen bonds to absolutely conserved tyrosine and tryptophan residues; these are essential to the photoprotective function of the OCP [22]. Binding to the protein changes the configuration of hECN: the terminal ring of hECN in the OCP is in an s-trans configuration, while hECN has an s-cis configuration in solution [20,21,23]. The change induced by interaction with the protein is associated with significant differences in the excited-state properties of hECN; the binding to the OCP activates the intramolecular charge transfer (ICT) state of hECN. In hECN this state, characteristic of carbonyl carotenoids in a polar environment [24,25], is observed exclusively in the OCP, underscoring the importance of the protein for tuning the excited-state properties of hECN.

The idea that the phycobilisome is the site of quenching in cyanobacteria was first suggested more than a decade ago [26], and involvement of the OCP was substantiated by the observation of increasing transcript levels of the OCP during exposure to intense light [27]. Another crucial observation was that the action spectrum of NPQ in *Synechocystis* matches the absorption spectrum of the OCP [28], as well as the finding that OCP mutants no longer show fluorescence quenching in response to blue light [29,30]. While these studies unequivocally identified the OCP as the key protein in photoprotection in cyanobacteria, they did not provide clues to the details of the photoprotective mechanism. In 2007, however, Wilson et al. [31] demonstrated that the OCP is a photoactive protein undergoing activation by blue-green light. The activated OCP, denoted OCP^r due to its characteristic featureless red-shifted absorption spectrum [31], can recover back to the resting OCP (usually denoted as OCP^o) by interaction with another protein, the Fluorescence Recovery Protein (FRP) [32,33]. Later, it was proved that the conjugated carbonyl group of hECN, and tryptophan and tyrosine residues that hydrogen bond to the carotenoid in the C-terminal domain, are required for OCP-mediated photoprotection [22,34].

Recently, two mechanisms for dissipation of energy by means of the OCP were proposed. Tian et al. [35] applied time-resolved fluorescence spectroscopy to whole cells of *Synechocystis* and, by comparing data recorded for mutants lacking the OCP to mutants overexpressing the OCP, identified a bilin chromophore in the phycobilisome core, APC_{660}, as the site of quenching. Moreover, analysis of time-resolved fluorescence data showed that quenching occurs with a time constant of ~240 fs. The investigators concluded that such a fast quenching rate most likely occurs via electron transfer between APC_{660} and the hECN in the OCP. A somewhat slower quenching was recently reported by the same group for isolated OCP-phycobilisome complexes [36]. On the other hand, Berera et al. [37] carried out transient absorption experiments on isolated OCP and its activated form, OCP^r, and concluded that the activated form has a pronounced ICT state that serves as a quenching state, and that quenching occurs via energy transfer from the S_1 state of bilin. As pointed out recently [36], it is obvious that the quenching mechanism is the same in vitro and in vivo, but it remains an open question whether electron transfer or energy transfer is responsible for the quenching.

Here we apply transient absorption spectroscopy in the near-IR region to determine the S_1 energy of hECN in solution and in the OCP to find out whether the interaction of hECN with the OCP and its activation to OCP^r alters the S_1 energy of hECN. Transient absorption spectra measured in the 900–1800 nm spectral region are usually dominated by the carotenoid S_1–S_2 transition. This allows measurement of the S_1 energy of carotenoids [38], a method successfully applied to reveal the S_1 energy of xanthophylls [39], linear carotenoids [40,41] and also carbonyl carotenoids [25]. Our results show that binding of hECN to the OCP alters S_1 energy of hECN as compared with that in organic solvent. Moreover, in the OCP^r the S_1 energy of hECN is significantly lower than in the OCP^o.

2. Materials and methods

2.1. Sample preparation

The OCP was isolated from the cyanobacterium *Arthrospira maxima* as described previously [20], dialyzed into buffer (5 mM Tris pH 8, 0.5 M EDTA, 80 mM NaCl), and stored in the dark at −50 °C. Prior to the experiments, the OCP was diluted in the same buffer to an optical density of ~0.1/mm at 495 nm. The sample was placed in a 2-mm quartz rotational cuvette (1.5 ml volume) and degassed by nitrogen. hECN was isolated from crude OCP as described earlier [23] and dissolved in methanol or n-hexane to yield optical density of ~0.2/mm at the absorption maximum (495 nm).

2.2. Ultrafast near-IR spectroscopy

The experimental setup consists of an amplified Ti:sapphire laser system operating at 5 kHz repetition rate that was used to pump two computer-controlled optical parametric amplifiers. One provided pulses that were used for excitation of the samples. The second parametric amplifier provided probe pulses for which the central wavelength was set by the computer in the 900–1800 nm spectral range. The probe beam was focused to a spot of 150 μm diameter, while the excitation spot was ~400 μm in diameter; the excitation intensity was kept below 10^{14} photons $pulse^{-1}$ cm^{-2}, and the intensity of the probe pulses were at least an order of magnitude lower for all experiments. The instrument response function was 120–150 fs depending on probe wavelength. Prior to interacting with the sample, the probe pulses were divided by a broadband 50/50 beamsplitter into the probe beam that overlapped with the pump beam at the sample, and a reference beam. The relative delay between pump and probe pulses was controlled by an optical delay line and their mutual polarization was set to the magic angle (54.7°). A 2-mm path rotating cell spinning at a rate sufficient to avoid exposure of the sample to multiple laser shots was used for the measurements. After passing through the sample, the probe and the reference beams were brought to the slit of a single-grating monochromator and finally detected by two germanium photodiodes. Since this arrangement does not allow broadband detection of the whole transient absorption spectra, kinetics were measured for a number of wavelengths (~70) spanning the 900–1800 nm spectral region and, after aligning the time zero of the individual kinetics to account for the chirp, the transient absorption spectra at the desired delay time were reconstructed from the kinetics.

3. Results

Absorption spectra of hECN dissolved in n-hexane and methanol as well as bound to the OCP are shown in Fig. 1. Changing solvent polarity produces the typical effects observed for many carotenoids with conjugated carbonyl groups, loss of vibronic structure and extension of absorption to longer wavelengths in polar solvents [25]. The 0–0 band of the S_0–S_2 transition remains unaffected by solvent polarity and peaks at 480 nm in both solvents. Upon binding of hECN to the OCP, the entire absorption spectrum is red-shifted; the 0–0 band at 495 nm and the resolution of vibrational bands is markedly larger than in organic solvent, indicating a locking the hECN in the OCP's binding pocket. This locking forces the terminal ring containing the carbonyl group into s-trans conformation [20,21], leading to linearization of the conjugated chain, which results in the well-resolved vibrational bands of hECN in the OCP [23].

It should be noted that the absorption spectrum of hECN in the OCP does not resemble a typical carotenoid absorption spectrum. The hECN in the OCP has its absorption maximum at the 0–0 band; in contrast essentially all absorption spectra of carotenoids in solution reported to-date have absorption maximum at the 0–1 vibrational

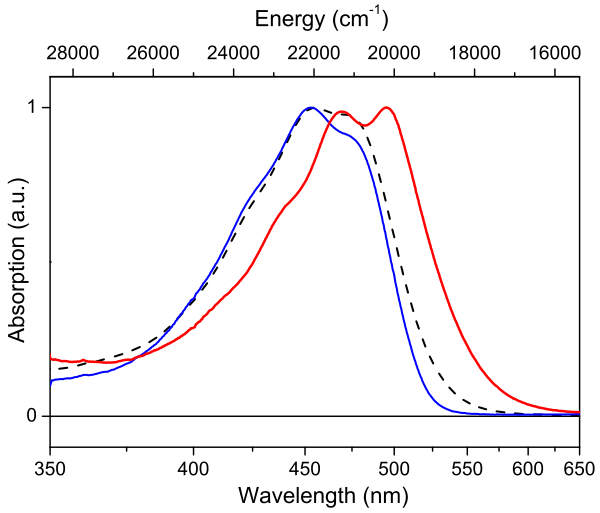

Fig. 1. Absorption spectra of hECN in n-hexane (thin solid, blue), methanol (dashed, black) and OCP (thick solid, red).

band [42]. Therefore, we deconvoluted the absorption spectrum of hECN in n-hexane and in the OCP into Gaussian bands (Fig. 2). While the absorption spectrum of hECN in n-hexane can be deconvoluted into a sum of vibrational bands, it is clear that deconvolution of the absorption spectrum of hECN in the OCP requires an additional band, that is broader than the 'standard' vibrational bands and peaks at

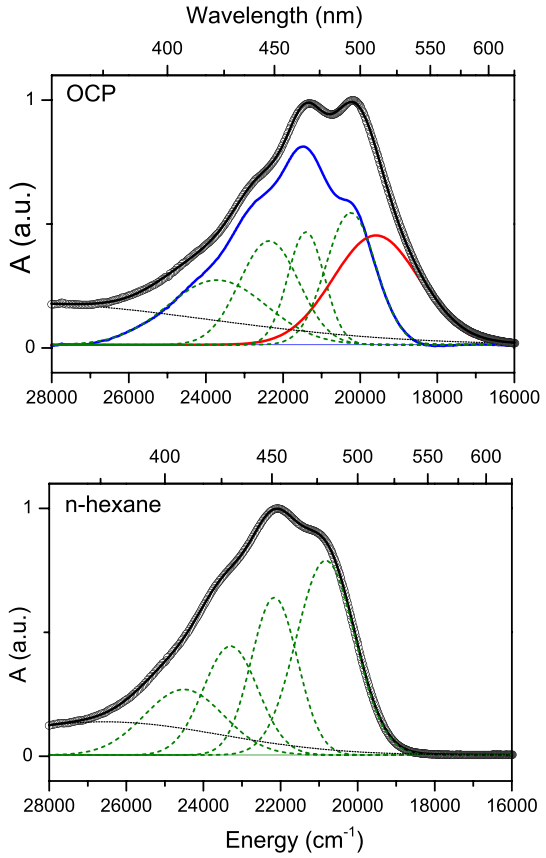

Fig. 2. Deconvolution of absorption spectra of hECN in the OCP (a) and in n-hexane (b). In the OCP, the red spectrum is due to OCP^r while the blue spectrum, obtained by subtraction of the OCP^r band from the OCP absorption spectrum, is the estimated absorption spectrum of OCP^o.

19,600 cm^{-1} (510 nm). This band is remarkably similar to the absorption spectrum of the activated OCP^r [31], suggesting that an OCP sample exposed to light at room temperature always contains some fraction of activated OCP^r. Since activation of the OCP occurs upon illumination by blue-green light and the activated OCP^r recovers in a few minutes in darkness at room temperature [31], it is expected that at ambient light there will be an equilibrium established between the OCP^o and OCP^r. The blue curve in Fig. 2 is the absorption spectrum of the OCP after subtraction of the red band (presumably due to OCP^r) and should therefore correspond to non-activated OCP^o.

In order to obtain information about the S_1 energy of hECN in various environments, we have recorded transient absorption spectra in the 800–1800 nm spectral region, which contains transient signals associated with the S_1–S_2 transition [39,40]. hECN was excited at 490 nm (in n-hexane or methanol) or 495 nm (in the OCP), wavelengths close to the 0–0 maximum of the S_0–S_2 transition for all three samples. It should be noted that 495 nm excites hECN in both OCP^o and OCP^r. Near-IR transient absorption spectra, reconstructed from kinetics measured over the whole near-IR region, are shown in Fig. 3. The selected time delay of 1 ps assures that processes associated with S_2–S_1 internal conversion are finished and that the transient absorption spectrum is dominated by contributions from the S_1 state.

The near-IR transient absorption spectrum of hECN in n-hexane exhibits a distinct peak around 1550 nm accompanied by a weaker band centered at ~1280 nm. Fitting the transient spectrum to a sum of Gaussian bands (Supporting information, Fig. S1) reveals four peaks with maxima at 1530 nm (6540 cm^{-1}), 1246 nm (8020 cm^{-1}), 10,930 nm (9150 cm^{-1}), and 967 nm (10,340 cm^{-1}). The energy separation between the peaks, 1100–1400 cm^{-1}, matches the separation of vibrational bands in the absorption spectrum shown in Fig. 1, confirming the assignment of the near-IR transient signals to the S_1–S_2 transition of hECN. The near-IR transient absorption spectrum of hECN in methanol is comparable to that in n-hexane, except the individual peaks are broader and less resolved, which mirrors the polarity-induced changes observed in the absorption spectrum (Fig. 1). We note here that fitting of the near-IR transient spectra to a sum of Gaussian bands (Fig. S1) provides a good fit for only the two lowest vibrational bands peaking at 1550 nm (6450 cm^{-1}) and 1280 nm (7800 cm^{-1}). This is most likely due to the presence of a weak stimulated emission band associated with the ICT state in methanol. Its magnitude is too weak to generate a negative band in

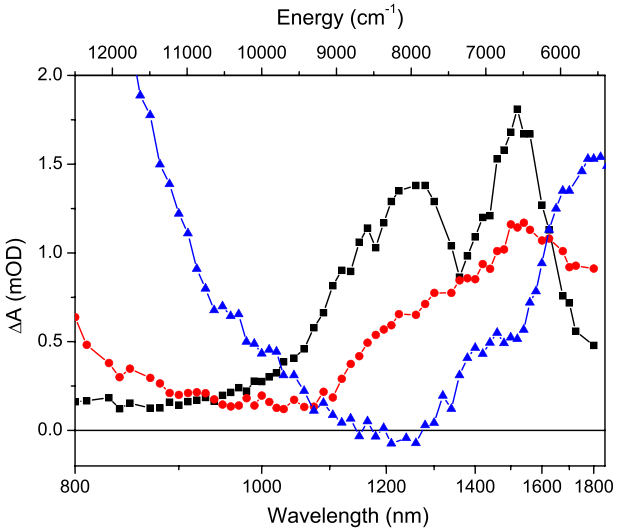

Fig. 3. Near-IR transient absorption spectra of hECN in n-hexane (black squares), methanol (red circles) and the OCP (blue triangles) measured at 1 ps after excitation at 490 nm (n-hexane, methanol) and 495 nm (OCP).

the near-IR, but it overlaps with the S_1–S_2 excited-state absorption in the 900–1100 nm region (Fig. 3); this precludes reproducing the spectrum only as a sum of vibrational bands of the S_1–S_2 transition. In fact, the influence of the ICT state may also be inferred from the magnitude of the signal at 800 nm. This signal is due to the red tail of the VIS excited-state absorption, which is associated with the ICT-like transition [23]. Thus, the stronger 800 nm signal in methanol is consistent with the presumed stimulated emission band in the near-IR.

Significant changes in the near-IR region are, however, observed when hECN is bound to the OCP. It is still possible to resolve two bands, peaking at ~1790 and ~1410 nm, but these bands are markedly red-shifted compared to those of hECN in methanol or n-hexane (see Fig. S1 for deconvolution of the most-red part of the transient absorption spectrum). Moreover, the signal around 1200 nm becomes slightly negative, as further confirmed (below) in kinetics recorded in that spectral region. This negative signal is reminiscent of the ICT emission observed for other carbonyl carotenoids [25]. It also further confirms the 'activation' of hECN's ICT state in the OCP that was proposed on the basis of transient absorption measurements in the visible spectral region [23]. A red-tail of the ICT-like excited-state absorption that peaks in the VIS region at 650 nm [23] is also observed as a strong signal in the high-energy part of the near-IR spectrum (Fig. 3).

Kinetics measured at the maxima of the lowest energy bands in the near-IR transient absorption spectra are shown in Fig. 4 for hECN in n-hexane, in methanol, and bound to the OCP. Since the S_1 lifetimes of 6.2 ps (n-hexane, methanol) and 3.3 ps (OCP) obtained from fitting the kinetics matches those reported in the visible spectral region [23], we can safely conclude that the signal in the near-IR region is indeed due to the S_1–S_2 transition of hECN. It should be noted that while hECN in n-hexane exhibits a single-exponential decay characterized solely by the 6.2 ps decay component, three components are necessary to fit the decay of hECN in the OCP. Besides the 3.3 ps component associated with the S_1 lifetime, an additional component of 0.9 ps must be included to fit the kinetics. As reported earlier, this component is also present in the visible spectral region [23,31] and it is more pronounced when the excitation wavelength is shifted to the red tail of absorption spectrum of hECN in the OCP [23]. Thus, it is likely that while the 3.3 ps component is associated with the OCP^o, the 0.9 ps component is characteristic of S_1/ICT lifetime of the activated the OCP^r. This hypothesis is further supported by recent transient absorption data recorded for the OCP immediately after illumination by blue-green light (containing almost exclusively activated OCP^r) [37]. These data demonstrate that the OCP^r has a dominating decay component of 0.6 ps, confirming that the shorter component is indeed due to the OCP^r. Thus, the OCP^o and the OCP^r can also be distinguished by their different S_1/ICT lifetimes. Moreover, the initial part of the decay requires fitting an ultrafast component with a time constant <100 fs. Since this component matches the S_2 lifetime of hECN in the OCP (see below), it indicates that the excited state absorption associated with S_2–S_N transition extends far beyond 1500 nm for hECN in the OCP. The kinetics of hECN in methanol displays intermediate behavior; the S_1 lifetime is the same as in n-hexane, 6 ps, but since an additional 120 fs component is required to fit the initial part of the decay at 1540 nm, it suggests that the S_2–S_N transition in methanol also extends as far to the red as in the OCP.

The S_2 lifetime manifested as a decay of the S_2–S_N signal is more clearly demonstrated in kinetics measured in the spectral region where the S_2–S_N signal dominates, at 1020 nm for hECN in n-hexane and methanol, and at 1210 nm for hECN bound to the OCP (Fig. 5). It is clear that the S_2 lifetime of hECN is longest in n-hexane (170 fs), shorter in methanol (110 fs), and it is further shortened for hECN bound to the OCP (<100 fs). These values match the dynamics of the appearance of the corresponding S_1–S_N bands in the visible region [23]. However, the kinetics of hECN in OCP at 1210 nm demonstrate that the S_2 state decays to form a weak negative signal (see inset of Fig. 5), which decays with a time constant of 3.3 ps, signaling the presence of the ICT state in hECN bound to the OCP.

For hECN in the OCP, the kinetics at selected wavelengths throughout the near-IR region were fitted globally. Three time components, of amplitudes shown in Fig. 6, were necessary to obtain good fits of all kinetics. The shortest time constant, <100 fs, peaks around 1100 nm and its spectral profile matches that expected for the S_2–S_N transition [43], confirming that this component corresponds to the S_2 lifetime. The longest component, 3.3 ps that matches the S_1 lifetime of hECN in the OCP [23,31] dominates in the 1400–1800 nm spectral region, implying that the S_1–S_2 signal indeed extends beyond 1800 nm. Around 1200 nm, the 3.3 ps component has a negative amplitude due to the presence of ICT stimulated emission that is clearly visible in the kinetics shown in Fig. 5. The intermediate component of 0.9 ps follows the spectral profile of the 3.3 ps component. The similarity of the spectral profiles of the 3.3 and 0.9 ps components is reminiscent of the situation in the visible spectral region [23,31], implying that, assuming that the 3.3 and 0.9 ps components are due to the OCP^o and OCP^r, respectively, the

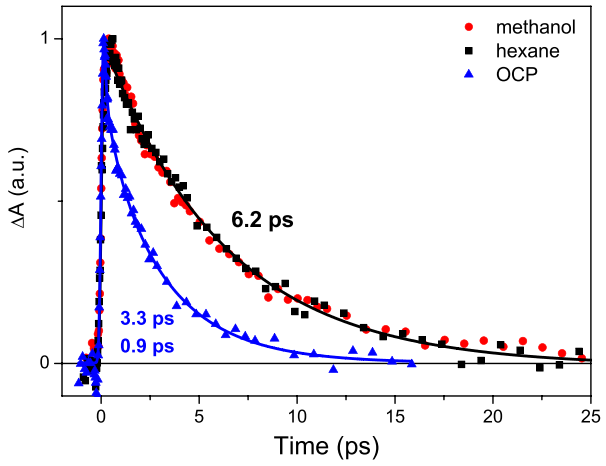

Fig. 4. Kinetics recorded at maximum of the 0–0 band of the S_1–S_2 transition at 1540 nm (n-hexane, methanol) and at 1830 nm (OCP). The time components extracted from fitting the kinetics are also indicated. Kinetics are normalized to the maximum, solid lines are fits. Fit of the data of hECN in methanol is omitted because it is essentially identical to the fit of hECN in n-hexane.

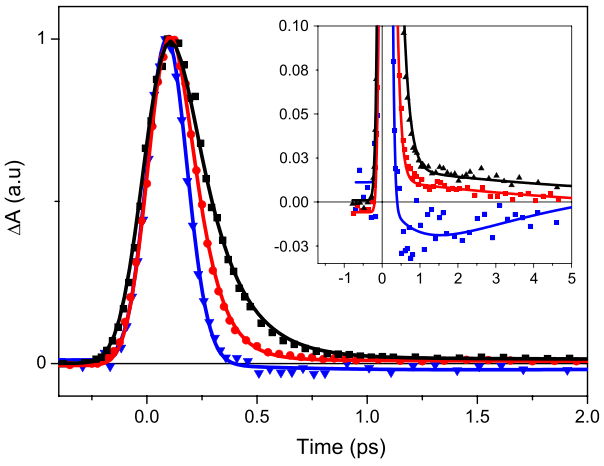

Fig. 5. Kinetics monitoring the decay of the S_2–S_N transition measured at 1020 nm for hECN in n-hexane (black squares) and methanol (red circles), and at 1210 nm for hECN in OCP (blue triangles). Inset shows magnification of the negative part of the kinetics measured for hECN in OCP. Kinetics are normalized to their maxima.

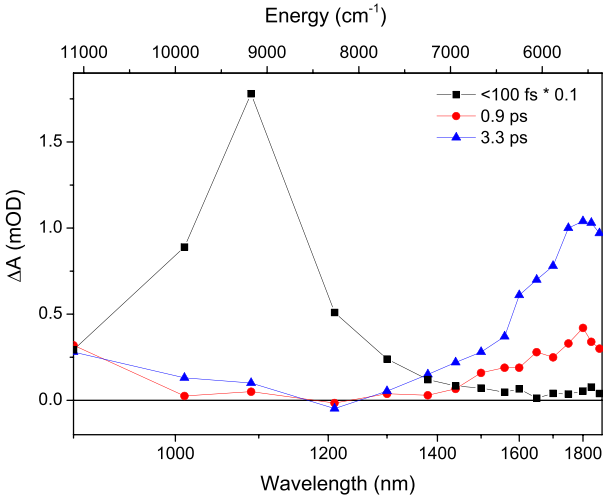

Fig. 6. Amplitudes of the pre-exponential factors of the three time components resulting from global fitting of kinetics of hECN in OCP. Note that the amplitude of the fastest component is divided by 10 to allow comparison with the other two.

spectral profiles of the S_1–S_2 transition of the OCP^o and OCP^r are not much different.

4. Discussion

Having established that the transient absorption spectra in the near-IR region (Fig. 3) indeed correspond to the S_1–S_2 transition, we may now proceed to determine the S_1 energy of hECN by subtracting the 0–0 energies of S_0–S_2 and S_1–S_2 transitions (Table 1) [39]. This procedure is most straightforward for hECN in n-hexane because the near-IR transient spectrum at 1 ps (Fig. 3) represents a pure S_1–S_2 transition, without any contribution from ICT stimulated emission. If we compare the absorption spectrum representing the S_0–S_2 transition (Fig. 1) with the spectral profile of the S_1–S_2 transition (Fig. 3), it is obvious that although vibrational bands are significantly more pronounced in the S_1–S_2 spectrum, a phenomenon observed earlier for other carotenoids [39,40], vibrational spacing between the individual vibrational bands in the S_1–S_2 spectrum (see Fig. S1) matches that in the absorption spectrum. Then, taking the energy 0–0 band of the S_0–S_2 transition from the absorption spectrum, 20,830 cm^{-1} (480 nm), and subtracting the energy of the lowest energy band in the S_1–S_2 spectrum, 6540 cm^{-1} (1530 nm), we obtain the S_1 energy of hECN in n-hexane of 14,300 cm^{-1}. It must be noted that using subtraction as described to obtain this value requires the assumption that the lowest energy transition in the near-IR transition absorption spectrum is the 0–0 band of the S_1–S_2 transition. Since our spectral window does not extend beyond 1850 nm, we cannot exclude the existence of another band with an even lower energy. This would imply that the 6540 cm^{-1} band in Fig. 3 is the 0–1 vibrational band, and the corresponding S_1 energy would be one vibrational quantum higher, at ~15,600 cm^{-1}. Such S_1 energy is, however, much higher than for other carotenoids with comparable conjugation lengths [38], which supports the assumption that the 6540 cm^{-1} band in the near-IR transient absorption spectrum is indeed the 0–0 band. Thus, we conclude that hECN in n-hexane has S_1 energy of 14,300 ± 100 cm^{-1}.

Table 1
Energies of vibrational bands of the S_0–S_2 and S_1–S_2 transitions.

Band	n-Hexane [cm^{-1}]	Methanol [cm^{-1}]	OCP [cm^{-1}]
S_0–S_2			
Red[a]	–	–	19,590
0–0	20,830	20,850	20,240
0–1	22,160	22,170	21,400
0–2	23,300	23,320	22,360
S_1–S_2			
0–0	6540	6450	5590
0–1	8020	7800	7100
0–2	9150	–	–

[a] An additional band is necessary to fit absorption spectra of hECN in the OCP. See text for details.

The same analysis also holds for hECN in methanol. Since there are only small shifts of the spectral bands in S_0–S_2 and S_1–S_2 transitions (Table 1), taking the energy of the 0–0 band of the S_0–S_2 transition, 20,850 cm^{-1}, and subtracting the energy of the 0–0 band of the S_1–S_2 transition, 6450 cm^{-1}, we obtain an S_1 energy of 14,400 cm^{-1} that is within the error of ± 100 cm^{-1} the same as in n-hexane (14,300 cm^{-1}). This is in accord with previous reports of S_1 energies of carbonyl carotenoids [44], which showed that the S_1 energy is not affected by solvent polarity. However, it is interesting to note that hECN in organic solvent has an S_1 energy that is significantly higher than that of another carbonyl carotenoid, spheroidenone. The S_1 energy of spheroidenone, measured by the same method as described here, is ~13,000 cm^{-1} [25], although hECN and spheroidenone have identical S_1 lifetimes, ~6 ps. Instead, the S_1 energy of hECN is more similar to that of non-carbonyl carotenoids with much shorter conjugation, such as violaxanthin or neurosporene [38] which have an S_1 lifetime of 24 ps [39,45]. This again underscores the influence of the conjugated carbonyl group on the excited-state properties of long carbonyl carotenoids. Even though these carotenoids do not exhibit polarity-dependent S_1 lifetimes, a phenomenon characteristic of carbonyl carotenoids with conjugation length shorter than 10 [46,47], their S_1 lifetimes and energies do not follow the effective conjugation length as do non-carbonyl carotenoids, but rather depend upon the position of the C═O group with respect to the main conjugated chain [48,49]. Consequently, the S_1 energies of two carotenoids with identical S_1 lifetimes can differ significantly, providing that they have different structures.

Binding of hECN to the OCP leads to a significant red shift of both the S_0–S_2 and S_1–S_2 transitions. Moreover, as described above, the absorption spectrum consists of contributions from the OCP^o whose 0–0 band of the S_0–S_2 transition peaks at 20,240 cm^{-1} (494 nm), and from the activated OCP^r peaking at 19,590 cm^{-1} (Table 1). The red-shift of the S_0–S_2 transition of the OCP^o could be explained by linearization of the conjugated backbone of hECN in the OCP's carotenoid binding cleft [23], leading to a longer effective conjugation than in organic solvent and, consequently, to the red-shifted S_0–S_2 transition. Previously, by comparison to studies on the excited-state dynamics of the carbonyl carotenoid peridinin that showed that a fraction of molecules with red-shifted absorption spectrum are most likely due to hydrogen bonding to the carbonyl oxygen [50], a hypothesis was proposed to explain the two decay components in the OCP [23]. The even further red-shifted absorption spectrum of the OCP^r is related to the same effect. Accordingly, the OCP^o-to-OCP^r conversion would correspond to a light-induced formation/strengthening of the hydrogen bonds between the C═O group of the hECN and the conserved tyrosine and tryptophan residues that are both essential for activation of the OCP [22].

While the red-shift of the S_0–S_2 transition of hECN in the OCP can be explained, the red-shift of the S_1–S_2 transition is difficult to account for. Both linearization of hECN in the binding cleft and the presumed hydrogen bonding in the OCP^r extends the effective conjugation of hECN; carotenoids with longer conjugation should have an S_1–S_2 transition slightly blue-shifted compared to the shorter ones [39,51]. Thus, hECN in the OCP would be expected to show a blue-shifted S_1–S_2 transition as compared to hECN in organic solvent. However, even though the high-energy part of the S_1–S_2 transition is masked by the ICT stimulated emission, the transient absorption spectrum shown in Fig. 3 allows

identification of two bands (see Fig. S1 for the deconvolution), at ~7100 cm^{-1} (1410 nm) and ~5590 cm^{-1} (1790 nm) that can be assigned to the 0–1 and 0–0 vibrational bands of the S_1–S_2 transition, respectively.

To estimate the S_1 energy of hECN in the OCP, it is important to realize that the spectral profiles of the 0.9 and 3.3 ps time components are very similar in the near-IR (Fig. 6). Since we assign the 3.3 and 0.9 ps components to the OCP^o and the OCP^r, respectively, it means that both have comparable spectral profiles for the S_1–S_2 transition, whereas the S_0–S_2 transition of the OCP^r is red-shifted by ~650 cm^{-1} (Table 1, Fig. 2). Thus, for the OCP^o, subtracting the 0–0 energy of the S_1–S_2 transition, 5590 cm^{-1}, from the 0–0 energy of the S_0–S_2 transition, 20,240 cm^{-1}, yields 14,650 cm^{-1} for the S_1 energy of hECN in the OCP^o. For hECN in the OCP^r, the energy of the 0–0 band of the S_1–S_2 transition is the same as in the OCP, but the S_0–S_2 transition has its peak at 19,590 cm^{-1} (Table 1, Fig. 2). Consequently, the S_1 energy of hECN in the OCP^r is ~14,000 cm^{-1}, which is lower than in the OCP^o.

Thus, by exciting a mixture of OCP^o and OCP^r at 495 nm, a wavelength that excites both forms approximately equally, and separating the contributions from the OCP^o and the OCP^r on the basis of their different S_1/ICT lifetimes, we conclude that while hECN in the OCP^o has S_1 energy of ~14,650 cm^{-1}, activation of the OCP decreases the S_1 energy of hECN to ~14,000 cm^{-1}. It must be noted that these values have error bars of about ± 200 cm^{-1} due to the uncertainty in deconvolution of the spectral bands in S_1–S_2 spectrum, and due to the uncertainty in the positions of the spectral bands in the amplitude spectra shown in Fig. 6 caused by the global fitting procedure. Despite this uncertainty, we can conclude that hECN in the OCP^r has a lower S_1 energy than in the OCP^o. This suggests that the change in interaction between the carbonyl group of hECN and the protein that likely occurs upon OCP activation [22,34] decreases the S_1 energy of hECN.

It is of course a question whether or not this effect has a role in the photoprotective function of the OCP. It is interesting that the values of the S_1 energy of hECN of ~14,650 cm^{-1} in OCP and of ~14,000 cm^{-1} in OCP^r are close to the S_1 energies of violaxanthin and zeaxanthin in solution [39]. Conversion of violaxanthin to zeaxanthin is the key process initializing the nonphotochemical quenching in plants [8]. Perhaps the OCP activation could be viewed as a simplified version of the xanthophyll cycle; while the xanthophyll cycle requires interconversion of two different carotenoids, in the OCP the comparable change in the S_1 energy is achieved via light-induced changes of the hECN-protein interaction.

Our results, however, cannot directly account for the quenching mechanism. Although it is tempting to speculate that the lower S_1 energy of hECN in the OCP^r may provide favorable spectral overlap to facilitate quenching by energy transfer while the higher S_1 energy in the OCP^o prevents this process (a mechanism called molecular gear shift proposed many years ago to explain nonphotochemical quenching in plants [52]), it is obvious that the mechanism is more complicated. First, it was shown that only OCP^r can bind to phycobilisomes [33], thus OCP^o likely never interacts with the quenching site. Consequently, the S_1 energy of hECN in OCP^o is irrelevant to the quenching mechanism. Second, it was recently shown that a bilin chromophore in the core of the phycobilisome, allophycocyanin emitting at 660 nm (APC_{660}), is the quenching site both in vivo [35] and in the isolated phycobilisome-OCP complexes [36]. Thus, the energy of the state that is to be quenched is larger than 15,000 cm^{-1}, implying that the S_1 energies of hECN in both OCP^o and OCP^r are presumably low enough to quench the APC_{660}. It is therefore possible that the down-shift of the S_1 energy of hECN upon OCP activation is only a side effect caused by local structural changes during the OCP^o-to-OCP^r conversion and is not directly related to the quenching mechanism. Yet, as also pointed out for the violaxanthin/zeaxanthin pair [53], it is often overlooked that when a carotenoid plays the role of energy acceptor, it is in the ground state prior to energy transfer. Then, the energy required to lift the carotenoid to the S_1 state should correspond to a vertical transition whose energy is larger than the 0–0 energies calculated here. It is therefore possible that the decrease of energy by 650 cm^{-1} upon activation of the OCP is just enough to open the energy transfer channel from APC^{660} to hECN in the OCP^r. Thus, future experiments on phycobilisome-OCP complexes to identify spectroscopic signatures of either hECN S_1 state (energy transfer mechanism) or hECN radical (electron transfer mechanism) could be very useful for elucidating the mechanism of OCP-mediated quenching.

Supplementary data to this article can be found online at http://dx.doi.org/10.1016/j.bbabio.2012.10.005.

Acknowledgements

Research in Czech Republic was supported by grants from the Czech Ministry of Education (MSM6007665808 and AV0Z50510513), and the Czech Science Foundation (202/09/1330). CAK is supported by the NSF (MCB 0851070).

References

[1] G.D. Scholes, G.R. Fleming, A. Olaya-Castro, R. van Grondelle, Lessons from nature about solar light harvesting, Nat. Chem. 3 (2011) 764–774.
[2] V.I. Novoderezhkin, R. van Grondelle, Physical origins and models of energy transfer in photosynthetic light-harvesting, Phys. Chem. Chem. Phys. 12 (2010) 7352–7365.
[3] T. Polívka, H.A. Frank, Molecular factors controlling photosynthetic light harvesting by carotenoids, Acc. Chem. Res. 43 (2010) 1125–1134.
[4] P. Palozza, N.I. Krinsky, Antioxidant effects of carotenoids in vivo and in vitro: an overview, Methods Enzymol. 213 (1992) 403–420.
[5] E. Peterman, F. Dukker, R. van Grondelle, H. van Amerongen, Chlorophyll-a and carotenoid triplet states in light-harvesting complex II of higher plants, Biophys. J. 69 (1995) 2670–2678.
[6] A. Gall, R. Berera, M.T.A. Alexandre, A.A. Pascal, L. Bordes, M.M. Mendes-Pinto, S. Andrianambinintsoa, K.V. Stoitchkova, A. Marin, L. Valkunas, P. Horton, J.T.M. Kennis, R. van Grondelle, A. Ruban, B. Robert, Molecular adaptation of photoprotection: triplet states in light-harvesting proteins, Biophys. J. 101 (2011) 934–942.
[7] P. Horton, A.V. Ruban, R.G. Walters, Regulation of light harvesting in green plants, Annu. Rev. Plant Physiol. Plant Mol. Biol. 47 (1996) 655–684.
[8] K. Niyogi, Safety valves for photosynthesis, Curr. Opin. Plant Biol. 3 (2000) 455–460.
[9] A.V. Ruban, R. Berera, C. Ilioaia, C.I.H.M. van Stokkum, J.T.M. Kennis, A.A. Pascal, H. van Amerongen, B. Robert, P. Horton, R. van Grondelle, Identification of a mechanism of photoprotective energy dissipation in higher plants, Nature 450 (2007) 575–578.
[10] N. Holt, D. Zigmantas, L. Valkunas, X.P. Li, K.K. Niyogi, G.R. Fleming, Carotenoid cation formation and the regulation of photosynthetic light harvesting, Science 307 (2005) 433–436.
[11] S. Bode, C.C. Quentmeier, P.N. Liao, N. Hafi, T. Barros, L. Wilk, F. Bittner, P.J. Walla, On the regulation of photosynthesis by excitonic interactions between carotenoids and chlorophylls, Proc. Natl. Acad. Sci. U. S. A. 106 (2009) 12311–12316.
[12] M.G. Müller, P. Lambrev, M. Reus, E. Wientjes, R. Croce, A.R. Holzwarth, Singlet energy dissipation in the photosystem II light-harvesting complex does not involve energy transfer to carotenoids, ChemPhysChem 11 (2011) 1289–1296.
[13] R. Berera, I.H.M. van Stokkum, S. D'Haene, J.T.M. Kennis, R. van Grondelle, J.P. Dekker, A mechanism of energy dissipation in cyanobacteria, Biophys. J. 96 (2009) 2261–2267.
[14] C.A. Kerfeld, Structure and function of the water-soluble carotenoid-binding proteins of cyanobacteria, Photosynth. Res. 81 (2004) 215–225.
[15] S. Bailey, A. Grossman, Photoprotection in cyanobacteria: regulation of light harvesting, Photochem. Photobiol. 84 (2008) 1410–1420.
[16] A. Wilson, C. Boulay, A. Wilde, C.A. Kerfeld, D. Kirilovsky, Light-induced energy dissipation in iron-starved cyanobacteria: roles of OCP and IsiA proteins, Plant Cell 19 (2007) 656–672.
[17] D. Kirilovsky, Photoprotection in cyanobacteria: the orange carotenoid protein (OCP)-related non-photochemical-quenching mechanism, Photosynth. Res. 93 (2007) 7–16.
[18] M.G. Rakhimberdieva, I.V. Elanskaya, W.F.J. Vermaas, N.V. Karapetyan, Carotenoid-triggered energy dissipation in phycobilisomes of *Synechocystis* sp PCC 6803 diverts excitation away from reaction centers of both photosystems, Biochim. Biophys. Acta 1797 (2011) 241–249.
[19] N.V. Karapetyan, Non-photochemical quenching of fluorescence in cyanobacteria, Biochem. Mosc. 72 (2007) 1127–1135.
[20] C.A. Kerfeld, M.R. Sawaya, V. Brahmandam, D. Cascio, K.K. Ho, C.C. Trevithick-Sutton, D.W. Krogmann, T.O. Yeates, The crystal structure of a cyanobacterial water-soluble carotenoid binding protein, Structure 11 (2003) 55–66.
[21] A. Wilson, J.N. Kinney, P. Zwart, C. Punginelli, S. D'Haene, F. Perreau, M.G. Klein, D. Kirilovsky, C.A. Kerfeld, Structural determinants underlying photoprotection in the photoactive orange carotenoid protein of cyanobacteria, J. Biol. Chem. 285 (2010) 18364–18375.

[22] A. Wilson, C. Punginelli, M. Couturier, F. Perreau, D. Kirilovsky, Essential role of two tyrosines and two tryptophans on the photoprotection activity of the orange carotenoid protein, Biochim. Biophys. Acta 1807 (2011) 293–301.
[23] T. Polívka, C.A. Kerfeld, T. Pascher, V. Sundström, Spectroscopic properties of the carotenoid 3′-hydroxyechinenone in the orange carotenoid protein from the cyanobacterium *Arthrospira maxima*, Biochemistry 44 (2005) 3994–4003.
[24] H.A. Frank, J.A. Bautista, J. Josue, Z. Pendon, R.G. Hiller, F.P. Sharples, D. Gosztola, M.R. Wasielewski, Effect of the solvent environment on the spectroscopic properties and dynamics of the lowest excited states of carotenoids, J. Phys. Chem. B 104 (2000) 4569–4577.
[25] D. Zigmantas, R.G. Hiller, F.P. Sharples, H.A. Frank, V. Sundström, T. Polívka, Effect of a conjugated carbonyl group on the photophysical properties of carotenoids, Phys. Chem. Chem. Phys. 6 (2004) 3009–3016.
[26] K. El Bissati, E. Delphin, N. Murata, A.L. Etienne, D. Kirilovsky, Photosystem II fluorescence quenching in the cyanobacterium *Synechocystis* PCC 6803: involvement of two different mechanisms, Biochim. Biophys. Acta 1457 (2000) 229–242.
[27] L. Huang, M.P. McCluskey, H. Ni, R.A. LaRossa, Global gene expression profiles of the cyanobacterium *Synechocystis* sp. strain PCC 6803 in response to irradiation with UV-B and white light, J. Bacteriol. 184 (2002) 6845–6858.
[28] M.G. Rakhimberdieva, I.N. Stadnichuk, T.V. Elanskaya, N.V. Karapetyan, Carotenoid-induced quenching of the phycobilisome fluorescence in photosystem II-deficient mutant of *Synechocystis* sp, FEBS Lett. 574 (2004) 85–88.
[29] A. Wilson, G. Ajlani, J.M. Verbavatz, I. Vass, C.A. Kerfeld, D. Kirilovsky, A soluble carotenoid protein involved in phycobilisome-related energy dissipation in cyanobacteria, Plant Cell 18 (2006) 992–1007.
[30] C. Boulay, L. Abasova, C. Six, I. Vass, D. Kirilovsky, Occurrence and function of the orange carotenoid protein in photoprotective mechanisms in various cyanobacteria, Biochim. Biophys. Acta 1777 (2008) 1344–1354.
[31] A. Wilson, C. Punginelli, A. Gall, C. Bonetti, M. Alexandre, J.M. Routaboul, C.A. Kerfeld, R. van Grondelle, B. Robert, J.T.M. Kennis, D. Kirilovsky, A photoactive carotenoid protein acting as light intensity sensor, Proc. Natl. Acad. Sci. U. S. A. 105 (2008) 12075–12080.
[32] C. Boulay, A. Wilson, S. D'Haene, D. Kirilovsky, Identification of a protein required for recovery of full antenna capacity in OCP-related photoprotective mechanism in cyanobacteria, Proc. Natl. Acad. Sci. U. S. A. 107 (2010) 11620–11625.
[33] M. Gwizdala, A. Wilson, D. Kirilovsky, In Vitro reconstitution of the cyanobacterial photoprotective mechanism mediated by the orange carotenoid protein in *Synechocystis* PCC 6803, Plant Cell 23 (2011) 2631–2643.
[34] C. Punginelli, A. Wilson, J.M. Routaboul, D. Kirilovsky, Influence of zeaxanthin and echinenone binding on the activity of the orange carotenoid protein, Biochim. Biophys. Acta 1787 (2009) 280–288.
[35] L.J. Tian, I.H.M. van Stokkum, R.B.M. Koehorst, A. Jongerius, D. Kirilovsky, H. van Amerongen, Site, rate, and mechanism of photoprotective quenching in cyanobacteria, J. Am. Chem. Soc. 133 (2011) 18304–18311.
[36] L.J. Tian, M. Gwizdala, I.H.M. van Stokkum, R.B.M. Koehorst, D. Kirilovsky, H. van Amerongen, Picosecond kinetics of light harvesting and photoprotective quenching in wild-type and mutant phycobilisomes isolated from the cyanobacterium *Synechocystis* PCC 6803, Biophys. J. 102 (2012) 1692–1700.
[37] R. Berera, I.H.M. van Stokkum, M. Gwizdala, A. Wilson, D. Kirilovsky, R. van Grondelle, The photophysics of the orange carotenoid protein, a light-powered molecular switch, J. Phys. Chem. B 116 (2012) 2568–2574.
[38] T. Polívka, V. Sundström, Ultrafast dynamics of carotenoid excited states — from solution to natural and artificial systems, Chem. Rev. 104 (2004) 2021–2071.
[39] T. Polívka, J.L. Herek, D. Zigmantas, H.E. Åkerlund, V. Sundström, Direct observation of the (forbidden) S1 state in carotenoids, Proc. Natl. Acad. Sci. U. S. A. 96 (1999) 4914–4917.
[40] T. Polívka, D. Zigmantas, H.A. Frank, J.A. Bautista, J.L. Herek, Y. Koyama, R. Fujii, V. Sundström, Near-infrared time-resolved study of the S1 state dynamics of the carotenoid spheroidene, J. Phys. Chem. B 105 (2001) 1072–1080.
[41] H. Cong, H.D.M. Niedzwiedzki, G.N. Gibson, A.M. LaFountain, R.M. Kelsh, A.T. Gardiner, R.J. Cogdell, H.A. Frank, Ultrafast time-resolved carotenoid to-bacteriochlorophyll energy transfer in LH2 complexes from photosynthetic bacteria, J. Phys. Chem. B 112 (2008) 10689–10703.
[42] G. Britton, S. Liaaen-Jensen, H.P. Pfander, Carotenoids Handbook, Birkhäuser, Basel, 2004.
[43] J.P. Zhang, L.H. Skibsted, R. Fujii, Y. Koyama, Transient absorption from the 1Bu+ state of all-trans-β-carotene newly identified in the near-infrared region, Photochem. Photobiol. 73 (2001) 219–222.
[44] D. Zigmantas, T. Polívka, R.G. Hiller, A. Yartsev, V. Sundström, Spectroscopic and dynamic properties of the peridinin lowest singlet excited states, J. Phys. Chem. A 105 (2001) 10296–10306.
[45] D.M. Niedzwiedzki, J.F. Koscielecki, H. Cong, J.O. Sullivan, G.N. Gibson, R.R. Birge, H.A. Frank, Ultrafast dynamics and excited state spectra of open-chain carotenoids at room and low temperatures, J. Phys. Chem. B 111 (2007) 5984–5998.
[46] D.M. Niedzwiedzki, N. Chatterjee, M.M. Enriquez, T. Kajikawa, S. Hasegawa, S. Katsumura, H.A. Frank, Spectroscopic investigation of peridinin analogues having different π-electron conjugated chain lengths: exploring the nature of the intramolecular charge transfer state, J. Phys. Chem. B 113 (2009) 13604–13612.
[47] F. Ehlers, D.A. Wild, T. Lenzer, K. Oum, Investigation of the S1/ICT-S0 internal conversion lifetime of 4′-apo-β-caroten-4′-al and 8′-apo-β-caroten-8′-al: dependence on conjugation length and solvent polarity, J. Phys. Chem. A 111 (2007) 2257–2265.
[48] P. Chábera, M. Fuciman, P. Hříbek, T. Polívka, Effect of carotenoid structure on excited state dynamics of carbonyl carotenoids, Phys. Chem. Chem. Phys. 11 (2009) 8795–8803.
[49] M.M. Enriquez, M. Fuciman, A.M. LaFountain, N.L. Wagner, R.R. Birge, H.A. Frank, The intramolecular charge transfer state in carbonyl-containing polyenes and carotenoids, J. Phys. Chem. B 114 (2010) 12416–12426.
[50] D. Zigmantas, R.G. Hiller, A. Yartsev, V. Sundström, T. Polívka, Dynamics of excited states of the carotenoid peridinin in polar solvents: dependence on excitation wavelength, viscosity, and temperature, J. Phys. Chem. B 107 (2003) 5339–5348.
[51] R.L. Christensen, M.G.I. Galinato, E.F. Chu, R. Fujii, H. Hashimoto, H.A. Frank, Symmetry control of radiative decay in linear polyenes: low barriers for isomerization in the S1 state of hexadecaheptaene, J. Am. Chem. Soc. 129 (2007) 1769–1775.
[52] H.A. Frank, A. Cua, V. Chynwat, A. Young, D. Gosztola, M.R. Wasielewski, Photophysics of the carotenoids associated with the xanthophyll cycle in photosynthesis, Photosynth. Res. 41 (1994) 389–395.
[53] A. Dreuw, Influence of geometry relaxation on the energies of the S1 and S2 states of violaxanthin, zeaxanthin, and lutein, J. Phys. Chem. A 110 (2006) 4592–4599.